Check for updates

Highly hydrophilic polyhedral oligomeric silsesquioxane (POSS)-containing aptamer-modified affinity hybrid monolith for efficient on-column discrimination with low nonspecific adsorption†

Yiqiong Chen, Dandan Zhu, Xinyue Ding, Guomin Qi, Xucong Lin [ID] * and Zenghong Xie*

A novel polyhedral oligomeric silsesquioxane (POSS)-containing aptamer-modified hybrid affinity monolith with excellent hydrophilicity and unique architecture without Si−OH groups is presented herein, and the nonspecific adsorption caused by the hydrophobic nature of the monolithic column or polar interaction with silanol groups is minimized. *Via* a simple "one-pot" procedure, hydrophilic monomers were facilely polymerized with the POSS-methacryl substituted (POSS-MA) and aptamer; a highly hydrophilic nature was obtained and the lowest contact angle of 11° was achieved. By using ochratoxin A (OTA) as the model analyte, highly selective recognition of OTA in the mixture was achieved and the control of nonspecific interactions and the cross-reactivity of OTB and AFB$_1$ were significantly improved. The recovery yield of OTB caused by nonspecific adsorption in the resultant monolith was only about 0.1% and remained steady even with the coexistence of a high OTB content (OTA : OTB = 1 : 50), which reached the best level to date and was obviously less than the 6.1% occurring in the hydrophobic POSS-containing control monolith, 8.3% in the POSS-PEI@AuNPs@aptamer affinity monolith and 18.7% in the silica-hybrid affinity monolith. When applied to wine and wheat samples, the nonspecific adsorption was significantly reduced and efficient discrimination of OTA was obtained with better results than that of the hydrophobic POSS-containing affinity column. This provides an attractive tool for minimizing the nonspecific adsorption for highly selective on-column recognition.

1. Introduction

The highly efficient discrimination of a target analyte is critical for on-column selective sample pretreatment. Aptamer-based affinity monolithic columns (Apt-MCs) that display fast mass transfer rates, good specificity and facile preparation have been widely studied and used intensively for the on-column specific extraction of a target analyte.[1–3] However, due to the nature of the stationary phase, nonspecific adsorption caused by hydrophobic adsorption or polar silanol groups exists and gives rise to possible interferences in the specific analysis of target analyte.[4,5] The development of certain ideal Apt-MCs to minimize the nonspecific adsorption is therefore meaningful.[6,7]

To date, many monolithic columns for the immobilization of aptamers, including organic polymer monoliths[8–11] and siloxane-based hybrid monoliths,[12,13] have been studied. Typical aptamer-modified polymer monoliths prepared by glycidyl methacrylate (GMA) and trimethylolpropane trimethacrylate (TRIM) or ethylenedimethacrylate (EDMA) have been developed for selective extraction.[8–10] Due to the hydrophobic nature of TRIM-based and EDMA-based polymer monoliths, serious nonspecific adsorptions might occur, which are mainly governed by the hydrophobic interactions between the target analyte and the monolithic surface.[11] Usually, improving the hydrophilic properties of the monolithic stationary phase is favourable. To achieve this goal, polar siloxane-based hybrid monoliths have been designed for grafting aptamers and are used for the online selective capture of the analyte.[14–16] However, the "sol–gel" procedure has to be involved for preparing the precursor, and thus polar Si–OH groups are produced and exposed on the resultant hybrid affinity monolith, which causes an uncontrolled interference in the specific capture of

Institute of Food Safety and Environment Monitoring, Fuzhou University, Fuzhou, 350108, China. E-mail: xulin@fzu.edu.cn, zhxie@fzu.edu.cn
†Electronic supplementary information (ESI) available. See DOI: 10.1039/c8an01890a

the analyte. In a typical case, Brothier *et al.*[14] fabricated aptamer-modified affinity hybrid monoliths by covalently binding the aptamer on a silica-hybrid matrix *via* the linking of glutaraldehyde. Due to the polar action of active Si–OH sites, the nonspecific interaction between the target analyte and the control column was notable with a high recovery of 14.1% (ochratoxin A, OTA), and the analogue OTB was adsorbed on the support with a high recovery of 18.7% (both the contents of OTA and OTB were 0.20 ng). These facts indicate that hydrophobic interactions and polar interactions are two major factors that cause nonspecific adsorption in the aptamer-based affinity monolithic columns.[11] The control of these two factors is essential for effectively restraining the nonspecific adsorption. As such, a hydrophilic aptamer-based affinity monolith without silanol groups is greatly desirable. Polyhedral oligomeric silsesquioxane (POSS), which possesses a well-controlled 3D framework[17,18] and has been widely used as a functional material for preparing stable hybrid monoliths without silanol groups,[19–22] has been taken into consideration. *Via* post-column modification, the POSS-polyethylenimine (PEI) matrix was used to immobilize the AuNPs@aptamer and the obtained aptamer-affinity monolith was used for the on-column recognition of OTA. The nonspecific adsorption of OTB was gained with the recoveries ranging from 8.3% to 12.0% (the contents of OTB ranged from 0.2 ng to 2.0 ng).[23] By using a "one-pot" strategy, another aptamer-modified POSS-containing hybrid monolith was reported,[24] in which the nonspecific interaction of OTB was gained with the recoveries ranging from 5.5% to 14.8%. In these cases, by means of the POSS-containing hybrid monolith, the "sol–gel" process was avoided and polar Si–OH groups that could cause nonspecific adsorption were eliminated. With the POSS-containing hybrid monoliths, the control of the nonspecific adsorption of the analogue OTB could be improved. However, due to the hydrophobic nature of POSS, all POSS-containing hybrid affinity monoliths reported previously were hydrophobic and the nonspecific interaction caused by hydrophobic interaction between the polymer matrix and the analyte could still be detected. So far, no highly hydrophilic aptamer-based hybrid affinity monolithic columns with low nonspecific adsorption have been reported. The development of a new highly hydrophilic aptamer-modified POSS-containing hybrid affinity monolith with high selectivity and low nonspecific adsorption would be promising.

Herein, a new POSS-containing aptamer-modified hybrid affinity monolith with excellent hydrophilicity and a unique architecture without Si–OH groups is presented. POSS-methacryl substituted (POSS-MA) with a rigid framework was employed to reinforce the mechanical stability of the monolithic column. *Via* a facile "one-pot" process, highly hydrophilic monomers, including 2-acrylamido-2-methyl propane sulfonic acid (AMPS) and *N,N'*-methylene-bisacrylamide (MBA), were polymerized with POSS-MA and aptamer (Scheme 1). The hydrophilic nature of the resultant monolith [poly(POSS-MA-*co*-MBA-*co*-AMPS-Apt), denoted as PMAA], was evaluated. Meanwhile, the hydrophobic affinity monolith poly
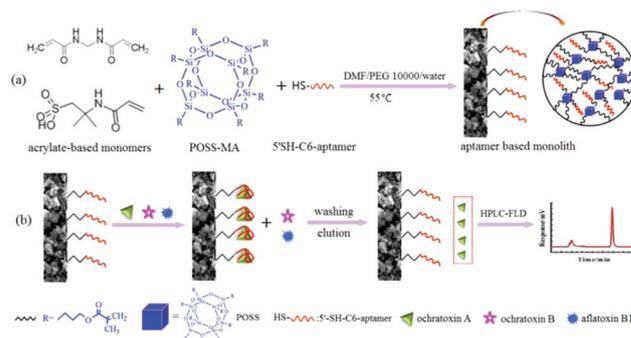
Scheme 1 Schematic of the preparation schemes for the PMAA monolithic column (a) and the diagram of affinity recognition of OTA (b).

(POSS-MA-*co*-EMDA-*co*-AMPS-Apt) [denoted as PEAA] was prepared as a comparison. By using OTA as the model analyte, the affinity performance of the PMAA monolith, including binding capacity, specificity, cross-reactivity and nonspecific adsorption were studied. Particularly, the selective capture of OTA was also tested in the mixture with a high OTB content (OTA : OTB = 1 : 50), and the nonspecific adsorption of OTB was successfully reduced. Applied to real wine samples, the discrimination of OTA was measured and acceptable results were achieved, which were better than that of the hydrophobic PEAA aptamer affinity monolith. This is an attractive tool for minimizing the nonspecific adsorption for highly selective extraction on-column.

2. Experimental

2.1 Chemicals and materials

The fused-silica capillary (100 μm i.d. × 365 μm o.d.) was obtained from Yongnian Optic Fiber Plant (Hebei, China). Polyhedral oligomeric silsesquioxane methacryl substituted (cage mixture, $n = 8$, POSS-MA) was purchased from Sigma-Aldrich (USA). 2-Acrylamido-2-methyl propane sulfonic acid (AMPS, 98%) was purchased from Tokyo Chemical Industry. Ochratoxin A (OTA, 98%), ochratoxin B (OTB, 98%), aflatoxin B1 (AFB$_1$, 98%) and *N,N'*-methylene-bis-acrylamide (MBA, ≥99.0%) were purchased from Aladdin Industrial Co. (Shanghai, China). Aptamer targeting ochratoxin A (5′-GATCGGGTGTGGGTG GCGTAAAGGGAGCATCGGACA-3′, denoted as Apt), and control oligonucleotide (5′-CTGGCC-CAGATTTTAAGGTGC GTAAAGAAAAAAAGT-3′, denoted as control ssDNA), both with the 5′-end modified by –SH through a C$_6$-spacer arm, were purchased from Sangon Biotech Co. (Shanghai, China). Binding buffer (BB) solution (10 mM Tris-HCl, 120 mM NaCl, 5 mM KCl and 20 mM CaCl$_2$, pH 8.50) and TE buffer solution (Tris-HCl 10 mM and EDTA 2.5 mM, pH 8.00) were prepared.

2.2 Preparation of PMAA and PEAA monoliths

The fused-silica capillary was pretreated and modified with γ-MAPS according to a previous report.[25] The mixture containing POSS-MA, monomers, aptamer solution, pore-forming

agents and AIBN with different compositions (as listed in Table S1†) were mixed and sonicated for 20 min to form a homogeneous solution. Then, the mixture was introduced into the capillary to an appropriate length with a syringe. The capillary was plugged at both ends with silicone rubber and submerged into a thermostatic bath at 55 °C for 12 h, followed by rinsing with a methanol–water solution to remove residual materials. The obtained PMAA affinity monoliths were stored at 4 °C in BB solution. The PEAA monolith was prepared by replacing the MBA monomer with ethylene dimethacrylate (EDMA). The control monolith was prepared with control ssDNA. The length of the PMAA affinity monolith was 10 cm.

2.3   Characterization of the PMAA monolithic column

The morphology was determined using scanning electron microscopy (Nova Nano SEM 230, USA). The energy-dispersive spectrum (EDS) was obtained by an electron probe microanalyzer (JEOL, JXA-8230, Japan). FT-IR spectra were obtained with a Fourier infrared spectrometer (Nicolet 6700, Nicolet Corp., USA). The contact angle (θ) of a water droplet on the monolithic surface was evaluated by optical contact angle measurement (HARKE-SPCAX1, Beijing).

2.4   Affinity recognition process

The on-column selective extraction of OTA was performed on the PMAA affinity column coupled with the HPLC-fluorescence detection system (LC-20A, Shimadzu, Japan) and the schematic diagram is shown in Fig. S1.† Briefly, 20 μL of OTA solution was percolated through the affinity column at a flow of 0.02 mL min^{-1}. Then, the affinity monolith was washed with BB solution at a flow rate of 0.1 mL min^{-1} to remove the residual OTA and ensure that no obvious OTA was further eluted by the BB solution. Finally, 20 μL of BB solution and 20 μL of elution solvent (ACN : TE = 30 : 70) were respectively used to elute OTA at a flow rate of 0.05 mL min^{-1} with a pressure drop of 250 psi.

2.5   Specificity, cross-reactivity and nonspecific adsorption analysis

The specificity towards OTA of the PMAA affinity monolith was evaluated by using the bare monolith and control monolith for comparison and then respectively applied to capturing OTA with the affinity recognition process mentioned above. Additionally, to evaluate the cross-reactivity of the PMAA affinity monolith, structural analogues such as OTB and AFB$_1$ acting as the model interfering toxins were chosen for measuring the cross-reaction on the three kinds of monoliths. To demonstrate the nonspecific interaction of the affinity monolith, the retention of OTB in the mixture (OTA : OTB = 1 : 1) on four affinity monolithic columns with different hydrophilic natures was studied. Particularly, the mixture with a high OTB content (OTA : OTB = 1 : 50) was employed to evaluate the nonspecific adsorption of OTB in the PMAA monolithic column.

2.6   Binding capacity of the PMAA monolithic column

The binding capacity of OTA on the PMAA monolith was measured by dynamic frontal analysis.[16] A 25 ng mL^{-1} solution of OTA was pumped through the PMAA monolith. The breakthrough curve was measured by plotting the peak area of OTA versus the volume of effluent solution. Toluene, a typically marked compound used for the void time in hydrophilic columns, was used to estimate the void volume. The binding capacity was obtained according to a previous report[24] and is shown in the ESI.†

2.7   Sample preparation

Red wine with the ethanol content of 11.5% was purchased from the local market; 10 mL of the red wine was degassed ultrasonically for 30 min, which had been previously cooled at 4 °C for 30 min. The pH of the wine samples was then adjusted to 8.5 with a 2 mol L^{-1} NaOH solution. After being filtered through the 0.22 μm membrane, the wine samples were spiked with OTA at some concentrations ranging from 0.10 ng mL^{-1} to 1.0 ng mL^{-1}. The fortified red wine samples were diluted with BB solution at a ratio of 1 : 1 (v/v).

Wheat samples were extracted according to a previous report.[26] Briefly, 5 g of finely ground wheat grain was mixed with 10 mL of water/ACN (40/60, v/v) in a centrifuge tube and then centrifuged at 4000 rpm for 20 min. The extract was filtered through the 0.22 μm membrane; then, 100 μL of resulting extract spiked with OTA at 1 μg kg^{-1}–6 μg kg^{-1} (equivalent to 0.50 ng mL^{-1} to 3.0 ng mL^{-1}) was diluted 10 times with the binding buffer solution. Finally, selective extraction was carried out via the process mentioned in section 2.4.

3.   Results and discussion

3.1   Characterization of the PMAA hydrophilic monolithic column

The preparation of the PMAA hydrophilic monolith is illustrated in Scheme 1. A series of optimizations was investigated and the procedures are shown in Table S1.† To form a homogeneous porous monolith with high hydrophilicity, polar monomers and aqueous aptamers were used, and water was used to dissolve these compounds. With the content of H$_2$O increasing from 5.0 to 10.0% (w/w) in the porogenic system, the permeability of the hybrid monoliths significantly decreased from 8.53×10^{-14} m^2 to 1.23×10^{-14} m^2 (Table S1†), which could cause a notable reduction in the mass transfer rate and elution efficiency of the resultant monoliths. Under the proper permeability of about 3.95×10^{-14} m^2, the effects of the POSS-MA monomer on the hydrophilic nature of the PMAA affinity monoliths were also investigated. As shown in Fig. 1, stable and homogeneous polymer morphologies were observed on the PMAA affinity monoliths with different contents of POSS-MA.

To clarify the degree of hydrophilicity of the affinity monolithic columns, the contact angle (θ) of a water droplet on the monolithic surface was evaluated. The water drop expanded rapidly on the surface of three flat sheets of monoliths with 2.5% POSS-MA (Fig. 1-a3), 5.0% POSS-MA (Fig. 1-b3) and 7.5% POSS-MA (Fig. 1-c3). The highly hydrophilic nature was
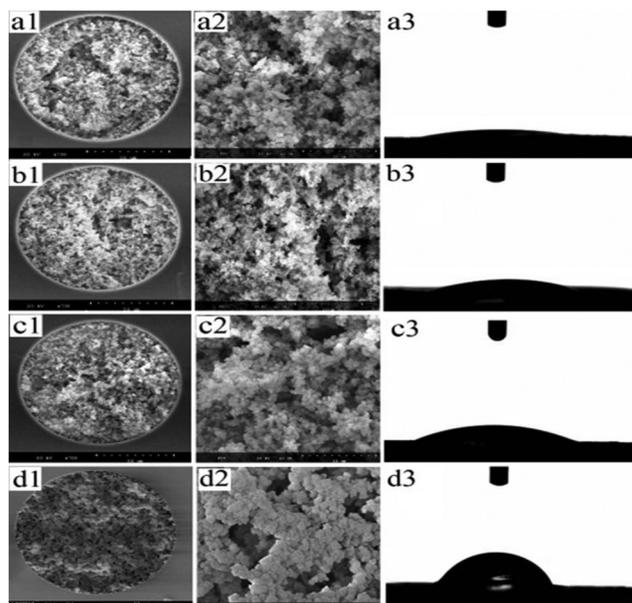
Fig. 1 SEM images of different monolithic columns and the contact angles of water on the flat sheets of monolithic surfaces: (a) PMAA column with 2.5% POSS-MA; (b) PMAA column with 5.0% POSS-MA; (c) PMAA column with 7.5% POSS-MA. (d) PEAA column; magnification times: (a1–d1) × 700, (a2–d2) × 2000.

observed with contact angles of 11°, 17° and 24°, respectively, while that of the hydrophobic PEAA affinity monolith reached up to 60° (Fig. 1-d3). The results indicated that the hydrophilic interaction interface of the PMAA affinity monolith with a low contact angle down to 11° was achieved by the introduction of highly hydrophilic monomers such as MBA and AMPS, which revealed the highest hydrophilic level among the current POSS-containing hybrid affinity monoliths and might be favourable for resisting the nonspecific adsorption caused by hydrophobic interactions.

To indicate that the aptamer was covalently attached to the hydrophilic POSS-containing hybrid monolithic column, the FT-IR spectrum of the monolithic material was obtained. As shown in Fig. 2, characteristic bands such as the CO–NH
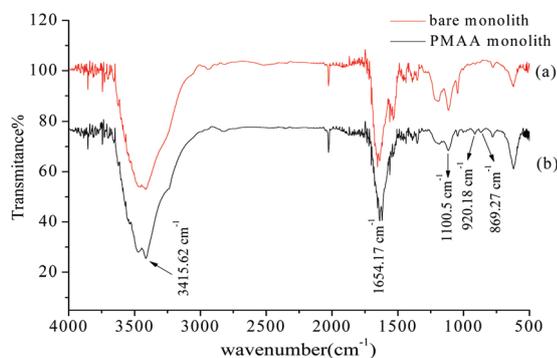

Fig. 2 FT-IR spectra of the bare monolith (a) and the PMAA monolith with 5.0% POSS-MA (b).

stretching vibration at 3415.62 cm^{-1} and 1654.17 cm^{-1}, and the Si–O band stretching vibration at 1100.5 cm^{-1} were observed in the bare hybrid monolithic matrix. New peaks emerging at 920.18 cm^{-1} and 869.27 cm^{-1} were observed and were attributed to the C–S vibration and the heterocyclic group, respectively, which revealed the immobilization of the thiolated-aptamer on the hybrid monolithic column *via* the "thiol–ene" click reaction.

EDS analysis was also carried out to investigate the surface composition and elemental states on the PMAA monolith. In Fig. 3-I, the composition profile of the blank monolith was different from the PMAA monolithic column. No obvious P signal could be measured on the blank monolith (in Fig. 3, I-a), while it was clearly observed on the PMAA affinity monolith column with the content of 0.13% (in Fig. 3, I-b); besides, a series of EDS mapping images of the main elements (C, O, N, Si, S and P) were measured (Fig. 3-II). The P signal was well-distributed and strong enough to be observed clearly, which could further confirm the successful modification of the aptamer.

3.2 Specificity of the PMAA monolithic column

3.2.1 Specific recognition of OTA. In this work, the typical OTA toxin (log $K_{O/W}$ = 4.6)[27] was used as the model analyte. The specificity recognition of OTA in the resultant PMAA monolith, bare monolith and ssDNA control monolith were evaluated. Recoveries of OTA in each effluent liquid of three stages (percolation, washing, and elution fraction, respectively) were measured and are shown in Fig. 4. The obvious response of OTA was detected in the percolation and washing fractions on both the bare monolithic column (Fig. 4A) and the control monolithic column (Fig. 4B), respectively. For the ssDNA control monolith, no obvious affinity chromatographic retention of OTA was observed, and almost all of the OTA was eluted
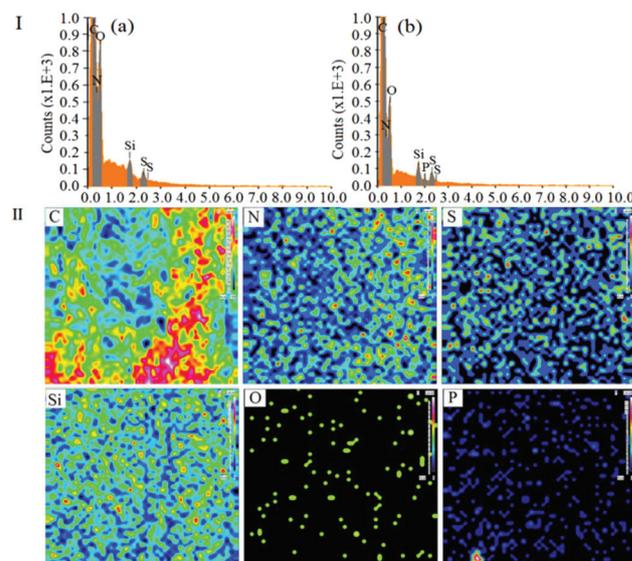

Fig. 3 EDS and EDS mapping images of the PMAA monolith. (I) EDS of the blank monolith (a) and PMAA monolith (b). (II) Mapping images of the PMAA monolith with 5.0% POSS-MA.
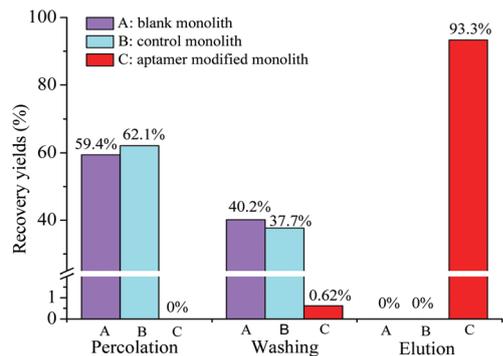
Fig. 4 Recoveries of OTA with various monoliths in the effluent liquid of different stages. (A) Bare monolith; (B) ssDNA control monolith; (C) PMAA monolith with 5.0% POSS-MA. The concentration of OTA was 10 ng mL^{-1}.

after the washing procedure. For the PMAA monolithic column, almost all of the OTA could be efficiently held in the percolation and washing fractions. Only 0.62% of OTA was detected in the washing fraction and a significant fluorescence response of OTA was obtained in the elution fraction (Fig. 4C) after switching to the ACN–TE eluent (ACN : TE = 30 : 70), thus confirming that the obtained PMAA hydrophilic monolith could effectively resist the nonspecific interaction between OTA and the highly hydrophilic hybrid monolithic matrix and remain highly specific to OTA.

3.2.2 Nonspecific adsorption. The nature of the support is a key parameter controlling the performances of the hybrid affinity monolithic column. To investigate the effect of the change in the polymerization solution on the nonspecific adsorption, three PMAA affinity monoliths with different POSS-MA contents and similar permeability were prepared. As seen from Fig. 5a–d, with the hydrophilic nature decreasing, the OTB content in the eluent solution in the percolation fraction decreased, and that of the washing fraction drastically
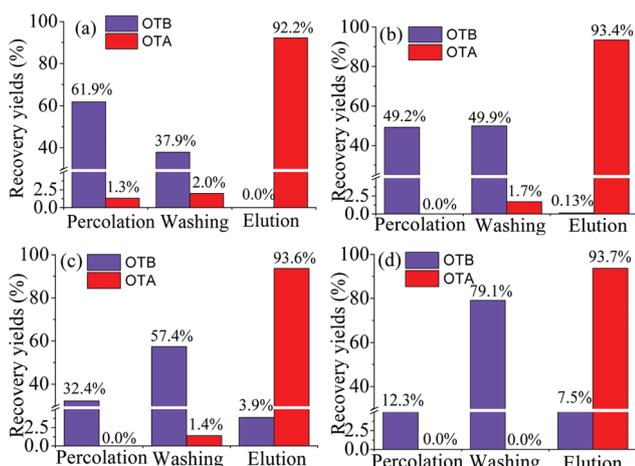

Fig. 5 Recoveries of OTA and OTB on affinity monoliths with different POSS-MA: (a) 2.5% POSS-MA; (b) 5.0% POSS-MA; (c) 7.5% POSS-MA; (d) PEAA monolithic column. The concentrations of OTA and OTB were both 10 ng mL^{-1}.

increased from 37.9% to 79.1%, which indicated that the high hydrophilicity could resist the nonspecific adsorption. The hydrophobic compounds adsorbed on the hydrophilic surface of the PMAA monolithic matrix could be easily eliminated with the binding buffer, and a small amount of OTA was detected in the washing fraction on the hydrophilic PMAA monolith (Fig. 5a–c), while that of the hydrophobic PEAA affinity monolith (Fig. 5d) was hard to remove due to the relatively strong unspecific adsorption. After the full washing procedure, the recoveries of OTA on the highly hydrophilic PMAA monoliths were about 92.2–93.6%, while the recoveries of OTB were 0, 0.13% and 3.9% in the mixture sample (OTA : OTB = 1 : 1), respectively.

Particularly, compared with the hydrophobic PEAA affinity monolith, a significant decrease in the recovery of OTB was achieved from 7.5% (Fig. 5d) to extremely low levels such as 0 or 0.13% in the PMAA monoliths that were prepared with 2.5% POSS-MA or 5.0% POSS-MA, respectively. As is known, the non-specific adsorption on the aptamer-based affinity monoliths might exist and the reasons mainly include two aspects; one is the hydrophobic nature of the acrylate-based polymer supports,[8–10] another is the polar Si–OH groups in silica-based monoliths.[14,16] In this work, by using hydrophilic monomers (MBA and AMPS) and rigid POSS chemicals, the resultant POSS-containing aptamer-based hybrid monolith (PMAA) could be prepared with a highly hydrophilic nature, and polar Si–OH groups were eliminated. Due to the highly hydrophilic nature and the special Si–O–Si framework, those two negative factors causing the undesirable adsorption of hydrophobic compounds were effectively controlled and extremely low non-specific adsorption of OTB was achieved in the PMAA hydrophilic monolith. In addition, with a lower content of POSS-MA, higher hydrophilicity was achieved, and the changes in the swelling properties of the PMAA monoliths became more obvious, which might weaken the affinity for interaction with the target OTA and lead to lower recovery (Fig. 5a). To gain the best specific interaction with OTA, the PMAA affinity monolith prepared with 5.0% POSS-MA possessing good mechanical stability and high hydrophilicity would be optimal, and the nonspecific adsorption recovery of OTB was only 0.13%.

To further evaluate the nonspecific adsorption of the PMAA monolith, the sample mixture with a high content of OTB (OTA : OTB = 1 : 50) was used for affinity analysis and that of the PEAA monolith was also studied as a comparison. As seen in Fig. 6a, by using the PMAA monolith, a good selective recognition of OTA was observed, and the recovery of OTB caused by the nonspecific adsorption was slight and only at 0.14% ± 0.2% (n = 3). With the hydrophobic PEAA monolith, the recognition of OTA was also observed and the recovery was similar to that in the PMAA monolith. However, significant adsorption of the coexisting compounds was detected in the PEAA monolith, which caused a rather high background fluorescence response. The recovery of OTB in the PEAA control monolith was obvious at 6.1% ± 1.0% (n = 3) (Fig. 6b), which was 40 fold greater than that in the PMAA monolith. The resultant highly hydrophilic PMAA monolith exhibited negligible nonspecific adsorption and a remarkable selectivity for OTA.
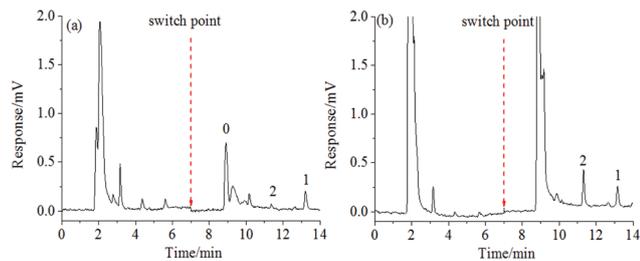
Fig. 6 Nonspecific adsorption of OTB on the PMAA monolith (a) and PEAA monolith (b) peak 0: background compound, peak 1: ochratoxin A, peak 2: ochratoxin B. The concentrations of OTA and OTB were 0.2 ng mL^{-1} and 10 ng mL^{-1}, respectively.

3.2.3 Cross-reactivity. To further test the selectivity of the PMAA monolith towards OTA, the cross-reactivity of other analogues such as OTB and AFB$_1$ were investigated and the resulting extraction profile is presented in Fig. 7. The obvious response of OTA, OTB and AFB$_1$ were observed in the percolation and washing fractions on the ssDNA control monolith (Fig. 7a), and scarcely any analytes were detected in the elution fraction. This means that three toxins could not effectively be absorbed on the hydrophilic ssDNA control monolith. However, the retention in the PMAA monolith was very different. As shown in Fig. 7b, almost all OTB and AFB$_1$ were removed through the percolation and washing processes, while extremely low or no OTA peaks were found. After switching, the OTA specifically captured by the aptamer bonded on
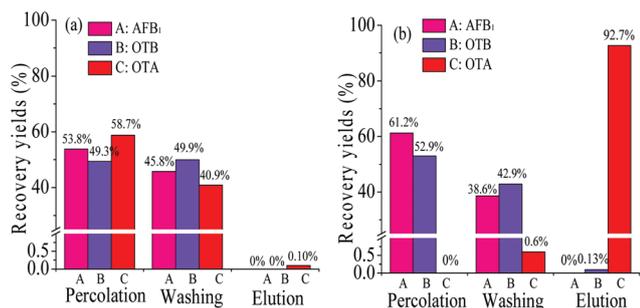
Fig. 7 Cross-reactivity of three toxins on the PMAA monolithic column targeting OTA; (a) ssDNA control monolith; (b) PMAA monolith. A: aflatoxin B1, B: ochratoxin B, C: ochratoxin A. The concentrations of OTA, OTB and AFB$_1$ were both 10 ng mL^{-1}.

the PMAA monolith could be effectively eluted, and thus the response of OTA was high and impressive, while few OTB and AFB$_1$ were observed on the PMAA monolith (Fig. 7b). The results clearly demonstrate that OTA was highly selectively captured on the PMAA monolith, while the cross-reactivity of OTB and AFB$_1$ could be ignored.

In summary, as shown in Table 1, when compared with the aptamer-modified columns previously reported,[14,23,24] the non-specific interactions in the obtained PMAA monolith were significantly reduced and possessed a better discrimination ability towards the target analyte. The highly hydrophilic PMAA monolithic column displays a highly selective and specific nature towards OTA with a quite low nonspecific adsorption.

3.2.4 Binding capacity. Binding capacity is defined as the maximum amount of target analyte captured by the aptamer modified monolithic column. The maximum binding capacity of OTA on the PMAA monolithic column was measured according to a previous report.[24] OTA solution (25 ng mL^{-1}) was pumped into the affinity capillary column to saturate the aptamer binding sites. As shown in Fig. S2,† the dynamic binding capacity Q_{max} in the PMAA monolithic column (10 cm-length) was calculated as 4.25 ng, which was similar to the affinity columns previously reported.[14,24]

3.2.5 Stability and lifetime. The mechanical stability of the PMAA monolith was also evaluated. As shown in Table S2,† with different mobile phases such as methanol, acetonitrile, water, elution solvent and BB solution, good mechanical stability was observed with an excellent linear relationship ($R^2 > 0.9973$) between the backpressure and flow rate of the mobile phase. The intra-day RSD ($n = 3$) and inter-day RSD ($n = 3$) on the PMAA affinity monolith were 1.5% and 2.0%, respectively. The PMAA monolith was rinsed with the binding solution after each analysis and stored at 4 °C. By using OTA as the model analyte (10 ng mL^{-1}), the PMAA monolith could be continuously used for 45 days with the recovery of OTA being above 90%, or 60 days with the recovery being above 84.5% (Fig. S3†).

3.3 Sample analysis

OTA is a naturally occurring mycotoxin that is frequently found in foods. To illustrate the selectivity of aptamer-based affinity columns towards OTA, red wine and wheat samples are often chosen,[26–29] and are thus studied here as the representative real samples.

Table 1 Nonspecific interaction in the PMAA affinity monolith as compared to previous reports

Affinity monolith	Recovery of OTA on control column (%, mean ± SD)	Recovery of OTB on the affinity column (%, mean ± SD)[a]	Ref.
Poly(TEOS-*co*-APTES)@aptamer	14.1% ± 9.5%	18.7% ± 6.0%	14
POSS-PEI@AuNPs@ aptamer	0.4% ± 0.3%	8.3% ± 0.3%	23
PEAA monolith	2.1% ± 0.5%	7.5% ± 0.2%[b]	This work
		6.1% ± 1.0%[c]	
PMAA monolith	None	0.13% ± 0.1%[b]	This work
		0.14% ± 0.2%[c]	

[a] The mass of OTB was 0.20 ng (equivalent to 10 ng mL^{-1} in 20 μL solution). [b] The mass ratio of OTA/OTB = 1 : 1. [c] The mass ratio of OTA/OTB = 1 : 50.
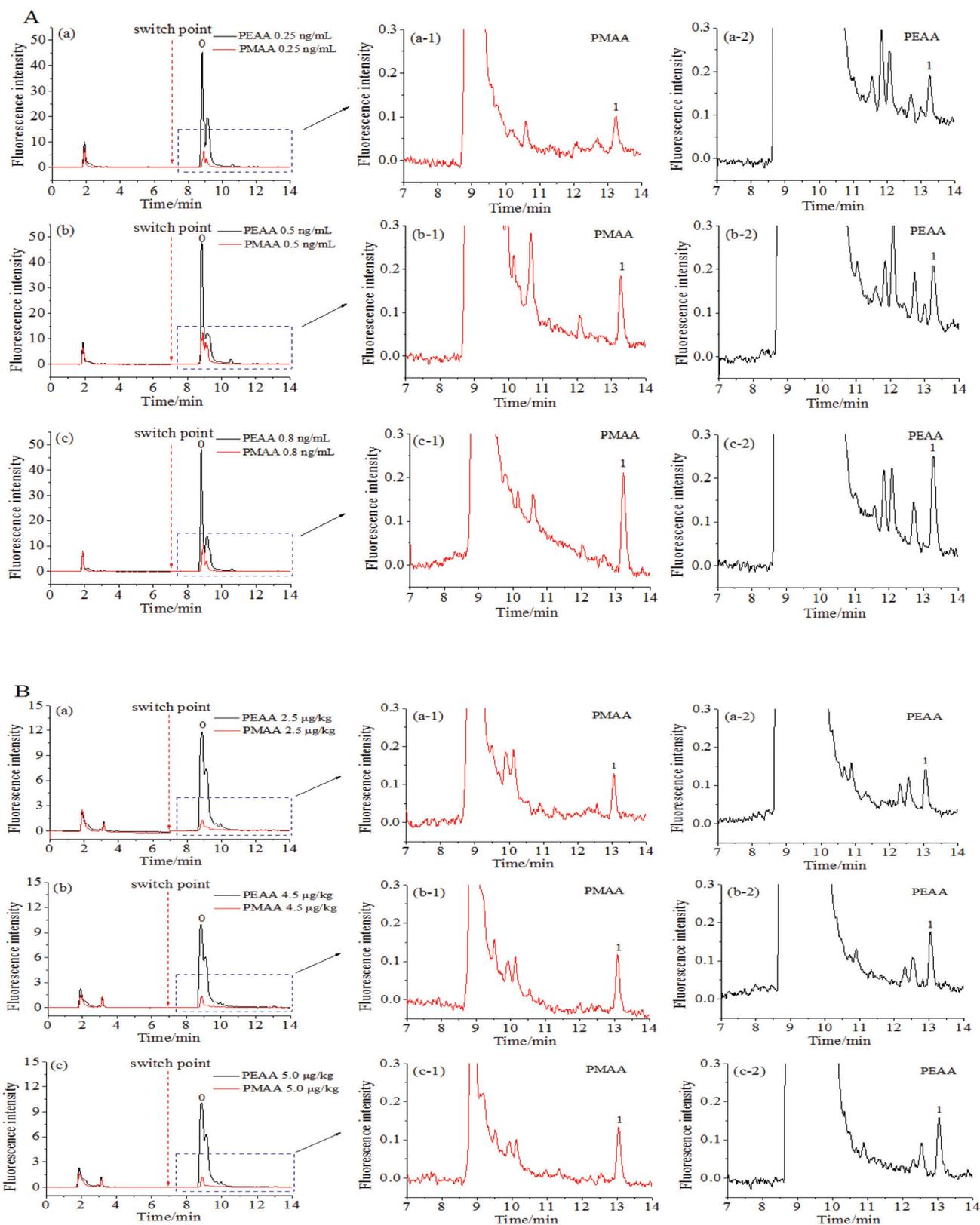
Fig. 8 Affinity recognition of OTA in red wine and wheat samples on a PMAA monolithic column and a PEAA monolithic column. (A) The concentrations of spiked OTA in red wine samples were (a) 0.25 ng mL^{-1}; (b) 0.50 ng mL^{-1}; (c) 0.80 ng mL^{-1}. (B) The concentrations of spiked OTA in wheat samples were (a) 2.5 µg kg^{-1}; (b) 4.5 µg kg^{-1}; (c) 5.0 µg kg^{-1}. Peak 0: background peak, peak 1: OTA.

The discrimination of OTA in red wine and wheat samples was evaluated with the obtained hydrophilic PMAA monolith. As shown in Fig. 8, the fluorescence response of background compounds in both kinds of food samples was rather high (black line) if the hydrophobic PEAA monolith was adopted, while that obtained with the hydrophilic PMAA monolith (red line) was drastically reduced. The adsorption of background compounds, such as anthocyanins and flavonoids in red wine[30] or dietary fiber, carbohydrates and protein in wheat samples,[31] was effectively inhibited on the hydrophilic PMAA monolith and could be more easily removed in the washing process when compared with the hydrophobic PEAA monolith. This indicated that the nonspecific adsorption of background compounds in wine and wheat samples could be significantly resisted on the PMAA hydrophilic monolith. Based on aptamers on the PMAA affinity monolith possessing a high specificity, OTA could be selectively extracted from the fortified samples (Fig. 8A/B, a1–c1). The chromatogram corresponding to the PMAA monolith was much better as compared to the hydrophobic PEAA monolith and possessed much less interference, which further confirmed that the highly hydrophilic PMAA affinity monolith facilitated the effective discrimination of OTA and the nonspecific interaction with the coexisting compounds was well controlled.

To express the capability of the PMAA hydrophilic affinity monolithic column for use in qualitative and quantitative analysis, the limits of detection (LOD) of OTA obtained in red wine and wheat samples were 0.10 ng mL^{-1} and 1.0 µg kg^{-1} (S/N = 3) respectively, while the limits of quantitation (LOQ) were 0.20 ng mL^{-1} and 2.0 µg kg^{-1} (S/N = 10), respectively. The recoveries of OTA from six fortified samples were further measured by using the hydrophilic PMAA and hydrophobic PEAA affinity monolith. In Fig. 8 and Fig. S4,† the obvious baseline drift and interference signals were both observed in the elution fraction by using the hydrophobic PEAA monolith, while the chromatograms obtained with the PMAA monolithic column possessed better baseline and symmetry of the retention peak. The chromatograms of elution solutions with the PMAA monolith (Fig. 8A/B, a1–c1) were more favorable for gaining accurate quantification as compared to the PEAA control monolith (Fig. 8A/B, a2–c2). As shown in Table 2, the recoveries of OTA obtained with the PMAA affinity monolith were satisfactory at 99.8 ± 1.3%–101.5 ± 3.9% (n = 3) for the spiked levels of OTA, 0.25 ng/mL–0.80 ng mL^{-1} in red wine, and 98.5 ± 2.8%–101.4 ± 2.6% (n = 3) for the spiked OTA at 2.5 µg kg^{-1}–5.0 µg kg^{-1} in wheat samples. For comparison, the recoveries of OTA on the hydrophobic PEAA monolith were measured and the fluctuation in recoveries was large in red wine (103.3 ± 5.7%–134.0 ± 5.4%

Table 2 Recoveries of OTA in red wine samples on different affinity monoliths

Sample	Concentration of OTA[a]	PMAA monolith		PEAA monolith	
		Average recoveries[b] (n = 3)	RSD% (n = 3)	Average recoveries[b] (n = 3)	RSD% (n = 3)
Red wine	0.25	101.5 ± 3.9%	3.9	134.0 ± 5.4%	4.0
	0.50	99.8 ± 1.3%	1.3	103.3 ± 5.7%	5.5
	0.80	100.4 ± 1.9%	1.9	105.3 ± 7.4%	7.1
Wheat	2.5	98.5 ± 2.8%	2.8	106.0 ± 4.6%	4.3
	4.5	101.4 ± 2.6%	2.5	103.1 ± 5.5%	5.3
	5.0	100.2 ± 1.8%	1.8	98.6 ± 4.3%	4.4

[a] The units of the spiking levels for undiluted red wine samples and wheat samples were ng mL^{-1} and µg kg^{-1}, respectively. [b] Average recoveries are presented as mean ± SD.

Table 3 Comparison of the results of OTA in real samples in this work with previous reports

Sample	Affinity material	Spiking level[a] (ng mL^{-1} or µg kg^{-1})	Recovery (%)	RSD	Ref.
Red wine	Aptamer-modified SPE column	2.0	93	—	27
	Aptamer-modified carbon nanohorn	8.06–201.5	93.0–104.9	2.1–4.7	28
	Aptamer-modified gold nanorods	2–20	92–118.2	—	32
	AuNPs@aptamer silica-hybrid monolith	0.5–5.0	90.3–91.6	2.7–3.4	33
	PEAA control monolith	0.25–0.80	103.3–134.0	4.0–7.1	This work
	PMAA monolith	0.25–0.80	99.8–101.5	1.3–3.9	This work
Wheat	Aptamer-modified SPE column	200–600	91.24–98.79	—	26
	Aptamer-modified SPE column	0.5–50	74–88	<6	29
	Aptamer-modified affinity column	2.5–25	72–81	3–7	34
	Aptamer-modified magnetic nanospheres	2.5–50	71.2–90.44	1.96–6.23	35
	PEAA control monolith	2.5–5.0	98.6–106.0	4.3–5.3	This work
	PMAA monolith	2.5–5.0	98.5–101.4	1.8–2.8	This work

[a] The unit of the spiking level for undiluted red wine samples and wheat samples were used as ng mL^{-1} and µg kg^{-1}, respectively.

(n = 3)), and relatively small in wheat (98.6 ± 4.3%–106.0 ± 4.6% (n = 3)). Particularly, an obvious deviation in OTA between the measured data and the spiked concentration in red wine samples with a low concentration of OTA at 0.25 ng mL^{-1} might be attributed to the serious baseline drift caused by the nonspecific adsorption in the PEAA monolith (Fig. S4-A-a-2†). The highly hydrophilic PMAA affinity monolith could facilitate the efficient discrimination of OTA and reduced nonspecific adsorption of coexisting compounds.

Compared with the aptamer-affinity materials reported previously,[26–29,32–35] the recoveries towards OTA in red wine and wheat samples were better (shown in Table 3). The highly hydrophilic PMAA monolith without Si–OH groups was more favorable for the selective recognition of OTA and achieving better quantification and recovery yields.

4. Conclusions

A novel highly hydrophilic POSS-containing aptamer-modified hybrid affinity monolith having a unique architecture without polar Si–OH groups was developed to minimize the nonspecific adsorption observed in common silica-hybrid monoliths. *Via* a simple "one-pot" procedure, the resultant monolithic column [poly(POSS-MA-*co*-MBA-*co*-AMPS-Apt), denoted as PMAA] was facilely prepared. A stable and homogeneous polymer morphology was obtained along with a highly hydrophilic nature and the lowest contact angle of 11° was achieved. Due to the high hydrophilicity of the PMAA monolithic column, a significant resistance of nonspecific adsorption was obtained. High selectivity towards trace OTA was achieved, and the control of nonspecific interactions and the cross-reactivity of OTB and AFB$_1$ could be well improved.

The recovery yield of OTB caused by nonspecific adsorption in the resultant PMAA monolith was only about 0.1% and remained steady even with the coexistence of a high content of OTB (OTA : OTB = 1 : 50), which reached the best level so far and was obviously less than the 6.1% occurring in the hydrophobic PEAA control monolith, 8.3% in POSS-PEI@ AuNPs@aptamer affinity monolith and 18.7% in the common silica-hybrid affinity monolith. Applied to real wine and wheat samples, the nonspecific adsorption was significantly reduced and the efficient discrimination of OTA was gained at 99.8 ± 1.3%–101.5 ± 3.9% (n = 3) for the spiked levels of OTA as 0.25–0.80 ng mL^{-1} in red wine, and measured as 98.5 ± 2.8%– 101.4 ± 2.6% (n = 3) for OTA at 2.5 μg kg^{-1}–5.0 μg kg^{-1} in wheat. The results were better than that of the hydrophobic PEAA control affinity columns or other aptamer-based affinity materials. This protocol could provide an attractive hydrophilic implement to effectively reduce nonspecific adsorption for the highly selective on-column recognition of the target analyte.

Conflicts of interest

There are no conflicts to declare.

References

1 N. Deng, Z. Liang, Y. Liang, *et al.*, *Anal. Chem.*, 2012, **84**, 10186–10190.
2 J. Ruta, C. Ravelet, J. Desire, *et al.*, *Anal. Bioanal. Chem.*, 2008, **390**, 1051–1057.
3 J. Masini and F. Svec, *Anal. Chim. Acta*, 2017, **964**, 24–44.
4 F. Brothier and V. Pichon, *Anal. Chim. Acta*, 2013, **792**, 52–58.
5 H. Lakhiaria, T. Okano, N. Nurdin, *et al.*, *Biochim. Biophys. Acta, Gen. Subj.*, 1998, **1379**, 303–313.
6 F. Du, L. Guo, Q. Qin, *et al.*, *TrAC, Trends Anal. Chem.*, 2015, **67**, 134–146.
7 V. Pichon, F. Brothier and A. Combès, *Anal. Bioanal. Chem.*, 2015, **407**, 681–698.
8 Q. Zhao, X. Li, Y. Shao, *et al.*, *Anal. Chem.*, 2008, **80**, 3915–3920.
9 Q. Zhao, X. Li, Y. Shao, *et al.*, *Anal. Chem.*, 2008, **80**, 7586–7593.
10 B. Han, C. Zhao, J. Yin, *et al.*, *J. Chromatogr. B*, 2012, **903**, 112–117.
11 Y. Chen, N. Deng, C. Wu, *et al.*, *Talanta*, 2016, **154**, 555–559.
12 Z. Wang, J. Zhao, H. Lian, *et al.*, *Talanta*, 2015, **138**, 52–58.
13 J. Zhao, Q. Zhu, L. Zhao, *et al.*, *Analyst*, 2016, **141**, 4961–4967.
14 F. Brothier and V. Pichon, *Anal. Bioanal. Chem.*, 2014, **406**, 7875–7886.
15 A. Marechal, F. Jarrosson, J. Randon, *et al.*, *J. Chromatogr. A*, 2015, **1406**, 109–117.
16 H. Jiang, J. Zhu, C. Peng, *et al.*, *Analyst*, 2014, **139**, 4940–4946.
17 R. Kannan, H. Salacinski, P. Butler, *et al.*, *Acc. Chem. Res.*, 2005, **38**, 879–884.
18 S. Phillips, T. Haddad and S. Tomczak, *Curr. Opin. Solid State Mater. Sci.*, 2004, **8**, 21–29.
19 J. Ou, Z. Zhang, H. Lin, *et al.*, *Anal. Chim. Acta*, 2013, **761**, 209–216.
20 X. Qiao, R. Chen, H. Yan, *et al.*, *TrAC, Trends Anal. Chem.*, 2017, **97**, 50–64.
21 M. Wu, R. Wu, R. Li, *et al.*, *Anal. Chem.*, 2010, **82**(13), 5447–5454.
22 H. Wang, J. Ou, Z. Liu, *et al.*, *J. Chromatogr. A*, 2015, **1410**, 110–117.
23 X. Yu, H. Song, J. Huang, *et al.*, *J. Mater. Chem. B*, 2018, **6**, 1965–1972.

24 Y. Chen, M. Chen, J. Chi, *et al.*, *J. Chromatogr. A*, 2018, **1563**, 37–46.

25 B. Xiong, L. Zhang, Y. Zhang, *et al.*, *J. High Resolut. Chromatogr.*, 2000, **23**, 67–72.

26 W. H. Ali and V. Pichon, *Anal. Bioanal. Chem.*, 2014, **406**, 1233–1240.

27 F. Chapuis-Hugon, A. Boisbaudry, B. Madru, *et al.*, *Anal. Bioanal. Chem.*, 2011, **400**, 1199–1207.

28 L. Lv, C. Cui, C. Liang, *et al.*, *Food Control*, 2016, **60**, 296–301.

29 G. A. De, M. Mckeague, J. D. Miller, *et al.*, *Food Chem.*, 2011, **127**, 1378–1384.

30 A. Hosu, V. M. Cristea and C. Cimpoiu, *Food Chem.*, 2014, **150**, 113–118.

31 J. Rosicka-Kaczmarek, A. Komisarczyk and E. Nebesny, *J. Cereal Sci.*, 2018, **81**, 37–43.

32 X. Xu, C. Xu and Y. Ying, *RSC Adv.*, 2016, **6**, 50437–50443.

33 J. Chi, M. Chen, L. Deng, *et al.*, *Analyst*, 2018, **143**, 5210–5217.

34 A. D. Girolamo, L. Le, G. Penner, *et al.*, *Anal. Bioanal. Chem.*, 2012, **403**, 2627–2634.

35 X. Wu, J. Hu, B. Zhu, *et al.*, *J. Chromatogr. A*, 2011, **1218**, 7341–7346.